CORROSION RESISTANCE OF UNS S31803 STAINLESS STEEL WELDED JOINTS

Paolo Ferro[1)], Jan-Olof Nilsson[2)], Franco Bonollo[1)]
[1)] Department of Engineering and Management, University of Padova, Stradella San Nicola 3, 36100 Vicenza, Italy
[2)] JON Materials Consulting, N. Hasselgatan 11, 811 35, Sandviken. Sweden

Received: 12.02.2018
Accepted: 28.05.2018

** Corresponding author: Prof. Paolo Ferro, Ph.D, Department of Engineering and Management, University of Padova, Stradella S. Nicola, 3 - 36100 Vicenza, ITALY, E-mail: ferro@gest.unipd.it, Mobile Phone: +39 334. 6957226, Phone: +39.0444.998727 - Fax: +39.0444.998884*

Abstract
The corrosion resistance of duplex stainless steel welded joints is affected by different parameters such as filler metal chemical composition, heat input, shielding gas composition and post welding heat treatment temperature. In most cases such parameters interact with each other so that it is very difficult to foresee their effect on corrosion resistance of welded joints without specific experimental tests. In this work the best combination of shielding gas composition and post welding heat treatment temperature that guarantees the corrosion resistance of the joint according to ASTM A932, method C, was found. Two shielding gases were tested during welding, Ar (100%) and a mixture of Ar (87%), He (10%) and N (3%), while the solution temperatures were 1050 °C and 1070 °C. It was found that only the samples welded with the mixture of Ar (87%), He (10%), N (3%) as shielding gas and solution heat treated at 1070 °C passed the corrosion test completely.

Keywords: Duplex Stainless Steel, Corrosion, Welding, Post Welding Heat Treatment, Shielding gas

1 Introduction

With very few exceptions, the welded joint is the Achilles heel and inferior to the parent metal with respect to mechanical properties and corrosion resistance [1-4]. During welding of duplex stainless steels, in particular during multi-pass welding, the formation of secondary austenite may lead to a significant reduction in pitting corrosion resistance [5]. Owing to the paucity of chromium, molybdenum and nitrogen, all of which contribute to corrosion protection, regions rich in secondary austenite are prone to corrosion attack [6]. Compared with primary austenite, the secondary austenite is formed at a lower temperature, where there is a thermodynamic driving force for forming additional austenite and where the equilibrium concentration of the above-mentioned elements is lower [7].
Early duplex stainless steels, such as for instance Sandvik 3RE60, were rich in ferrite and, therefore, not tough enough for many applications. This was even more pronounced in the welds since the reformation of austenite during welding was slow leading to unacceptably high volume fractions of ferrite. In modern duplex stainless steels it is customary to use a filler metal with a higher content of nickel than the parent metal to increase the austenite stability. However, nickel

DOI 10.12776/ams.v24i2.1073 p-ISSN 1335-1532
e-ISSN 1338-1156

alone is not sufficient to guarantee reformation of austenite during welding because of the short times involved [8]. As pointed out by Hertzman et al. [9] it is important to maintain a high concentration of nitrogen, which diffuses much faster than nickel and makes austenite reformation more efficient. Not only does nitrogen enhance the reformation of austenite but also helps to achieve equal corrosion resistance in austenite and ferrite.
Hence, it is quite essential to prevent nitrogen loss from occurring during welding. This is particularly a risk when the shielding gas is devoid of nitrogen. Because of this tendency, nitrogen is often added to the shielding gas. It is a delicate task to find a nitrogen concentration that is compatible with the nitrogen activity in the weld metal. Nitrogen also redistributes within the weld but the time available is short and there may not be sufficient time for all nitrogen to escape from the ferrite, which then becomes supersaturated. The formation of chromium nitrides in the ferrite is, therefore, a potential problem. Another potential problem is the formation of secondary austenite. In the present investigation, nitrogen loss and formation of secondary austenite are the central issues.

2 Materials and Methods

The joints under investigation were obtained from longitudinal hybrid Plasma-TIG welded pipes (external diameter 219 mm, thickness 12 mm and length 1196 mm). The pipe to be welded passes first under the plasma beam (with filler metal) and then under two TIG arcs (**Fig. 1a**). The first one, within the pipe, is used as root welding (without filler metal) and the second one, above the seam, is used as capping pass (CP) (with filler metal).

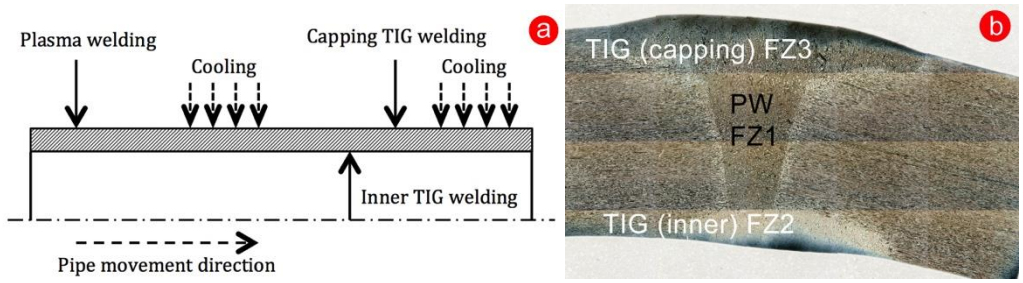

Fig. 1 Schematic of the hybrid Plasma-TIG welding operation (a) and macrograph of the weld bead (b)

The parent metal (PM) chemical composition matched that of the duplex stainless steel (DSS) UNS S31803 (**Table 1**) while the filler metal (FM) (ER2209) had a composition shown in **Table 2**.

Table 1 Chemical composition of the Parent Metal (wt. %)

C	Si	Mn	P	S	Cr	Ni	Mo	N	Fe
0.017	0.4	1.4	0.028	0.001	22.4	5.2	2.8	0.18	Bal.

Table 2 Chemical composition of the Filler Metal (wt. %)

C	Si	Mn	P	S	Cr	Ni	Mo	N	Cu	Co	Fe
0.01	0.51	1.64	0.017	<0.0005	22.89	8.59	3.04	0.15	0.13	0.057	Bal.

In order to guarantee an interpass temperature below 150 °C and avoid secondary phases precipitation, the pipe was cooled with a mixture of water (98%) and vegetable oil (2%) after both the plasma welding and the capping pass (**Fig. 1a**). In all the tests, the shielding gas used

DOI 10.12776/ams.v24i2.1073 p-ISSN 1335-1532
e-ISSN 1338-1156

during the inner welding was maintained always the same (95% Ar, 5% H). Hydrogen in shielding gas allows to increase the energy transferred by the arc to the joint and inhibits the oxides formation on the surface. However, because of its possibility to brittle the ferrite phase, its amount must be limited.

Two shielding gases were tested during plasma and capping TIG welding: Ar (100%) and a mixture of Ar (87%), He (10%) and N (3%) named in this work shielding gas 1 (SHG1) and shielding gas 2 (SHG2), respectively. SHG2 was designed to enhance a better-balanced microstructure above all in the HAZ (thanks to the presence of N [9]) and to increase the energy transferred to the weld pool thanks to the presence of He. After welding, a solution heat treatment was carried out on pipes using an induction heating. In order to evaluate the influence of post welding heat treatment (PWHT) parameters on corrosion resistance of the joints, two different solution temperatures were tested: 1050 °C and 1070 °C. The holding time at the maximum temperature (1050 °C or 1070 °C) was kept always the same (60 s). Because of their low thickness, the pipes reach the target temperature in few seconds. Furthermore, in order to prevent any secondary phases precipitation, they are immediately water-quenched at the end of the heating stage. After PWHT the pipes were pickled in a chemical solution containing HF (45 g/l) and H2SO4 (180 g/l) at a temperature of 45 °C for 6-8 h. Finally, the pipes underwent a passivation treatment in a solution containing HNO_3.

The microstructure of the samples was investigated by means of both optical microscope (OM) and environmental scanning electron microscope (ESEM) equipped with an energy-dispersive spectrometer (EDS). The samples observed with OM were etched by using a solution of H2O (80 ml), HCl (20 ml) and KHSO4 (1 g). Micrographs were quantitatively analysed by using the Leica QWin image analyser. The corrosion tests were carried out following the Standard ASTM A932, method C.

The PM was characterized by a balanced ferrite/austenite microstructure (52%/48%). **Table 3** summarized the welding parameters chosen on the base of welders experience. It is observed that because of the presence of He in SHG2, the heat input was lower when using SGH2 compared to SHG1.

Table 3 Welding parameters (welding speeds were 13 cm/min and 15 cm/min for pipes welded with SHG1 end SHG2, respectively)

	Plasma welding	Inner TIG welding	Capping TIG welding
Voltage (V)	34.4	18	16
Current (A)	250 (SGH1) 230 (SHG2)	200	320 (SGH1) 280 (SHG2)

3 Results

Figs. 2 and **3** shows the micrographs of the fusion zone (FZ) in the three main zones of the bead (**Fig. 1b**) of the as-welded joints: the upper zone, induced by the cosmetic TIG welding, the intermediate zone, induced by plasma welding (PW) and the inner zone induced by the TIG welding inside the pipe. In particular, **Fig. 2** shows the micrograph of the as-welded joint obtained with Ar as shielding gas, while **Fig. 3** the micrographs of the joint obtained with a mixture of Ar (87%), He (10%), N (3%) as shielding gas. Ferrite proportion was measured by image analysis and each value is the average of eight fields at 200 magnifications. Results of ferrite proportion in the as-welded joints as a function of shielding gas composition are summarized in **Fig. 4**.

DOI 10.12776/ams.v24i2.1073 p-ISSN 1335-1532
e-ISSN 1338-1156

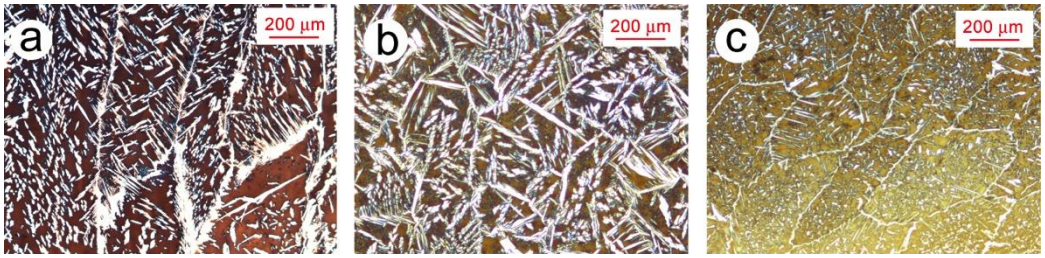

Fig. 2 Micrographs of fusion zone induced by TIG capping welding (a), Plasma welding (b), and inner TIG welding (c) (Fig. 1b); (as-welded joint, SHG1)

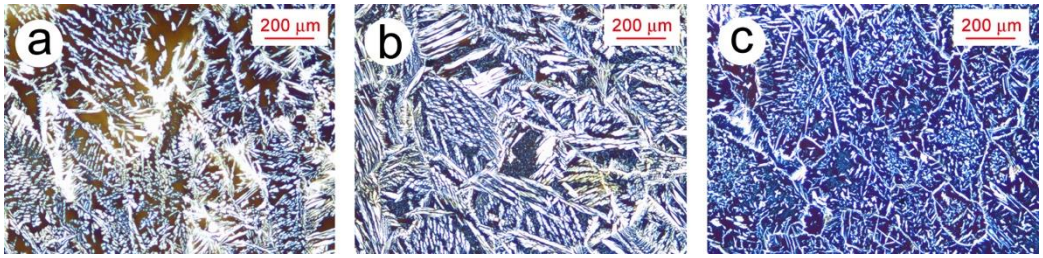

Fig. 3 Micrographs of fusion zone induced by capping TIG welding (a), Plasma welding (b), and inner TIG welding (c); (as-welded joint; SHG2)

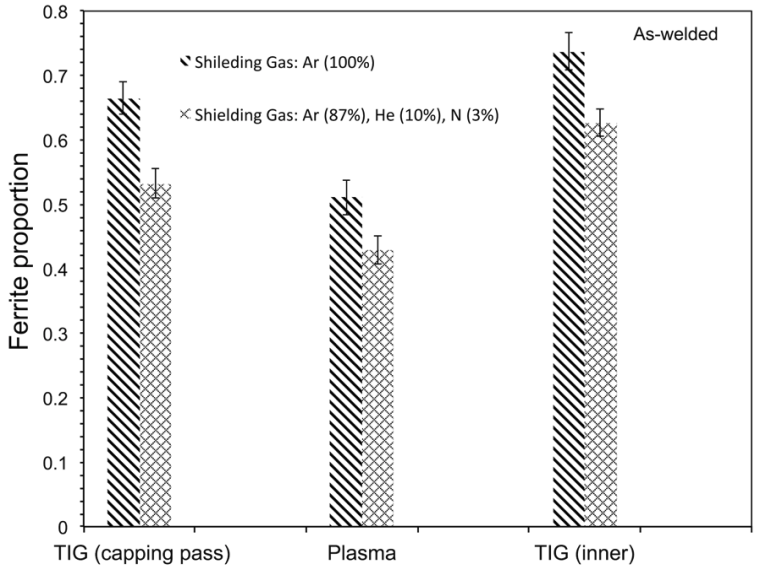

Fig. 4 Ferrite proportion in as-welded joints as a function of shielding gas

The micrographs of the FZ induced by the capping TIG pass after the solution heat treatment at 1050 °C and 1070 °C are shown in **Figs. 5** and **6**, respectively.

The results of ferrite quantification in the different zones of the bead as a function of shielding gas composition and solution temperature are summarized in **Fig. 7**. Thanks to the rapid heating and cooling, no secondary phases were detected in post-welding heat-treated joints [10, 11].

DOI 10.12776/ams.v24i2.1073 p-ISSN 1335-1532
e-ISSN 1338-1156

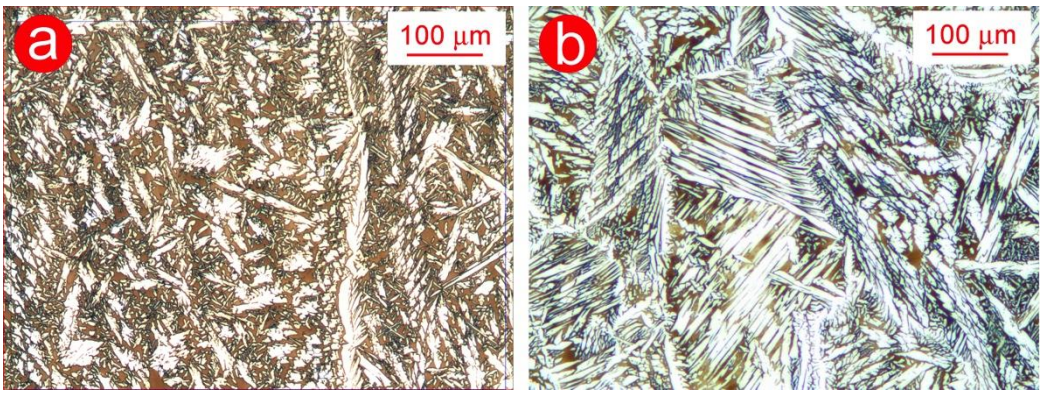

Fig. 5 Micrographs of the FZ (capping TIG pass) after solution heat treatment at 1050 °C. Shielding gas: a) SHG1; b) SHG2

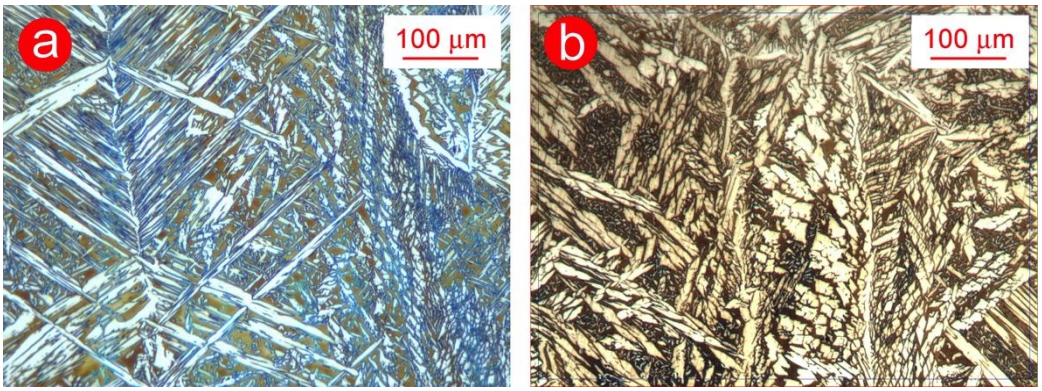

Fig. 6 Micrographs of the FZ (capping TIG pass) after solution heat treatment at 1070 °C. Shielding gas: a) SHG; b) SHG2

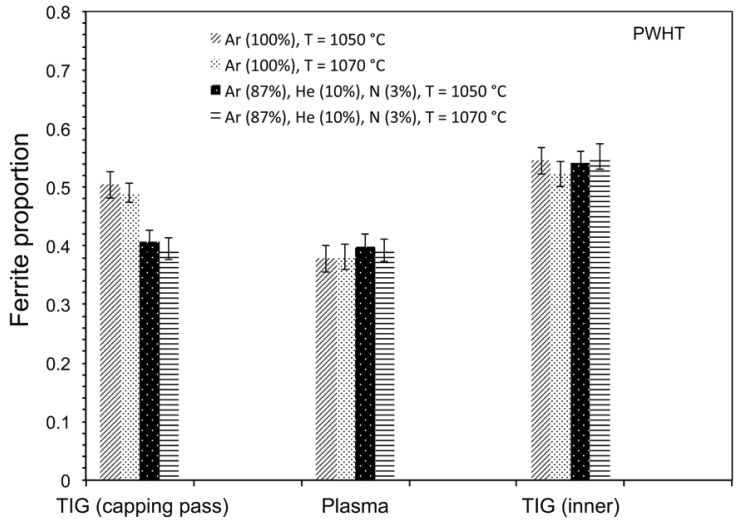

Fig. 7 Ferrite proportion in PWHT joints as a function of shielding gas chemical composition and solution temperature

DOI 10.12776/ams.v24i2.1073
p-ISSN 1335-1532
e-ISSN 1338-1156

Since the PWHT is become a common practice in industry that produces pipes in duplex and super-duplex stainless steel, the corrosion tests were carried out only on heat-treated samples. Comparison between heat-treated and as-welded joints corrosion properties can be found in literature [12-14]. Four samples for each combination of solution temperature and shielding gas composition were tested. **Fig. 8** summarized the results obtained. A straight line is also plotted which defines the exceeded limit of the test (weight loss, 1 g/m^2). It is observed that only the samples coming from pipes welded with the mixture of Ar (87%), He (10%), N (3%) as shielding gas and solution treated at 1070 °C have completely passed the corrosion test. Furthermore, shielding gas composition seems to have a major influence on corrosion resistance of the joint than the solution temperature. The weakest area of the weld bead was the FZ induced by the capping TIG pass. In order to detect which phase is attacked by corrosion first, a further corrosion test was performed according to ASTM A923, method C, but in this case the test duration was reduced to 6 h compared to the standard 24 h. The sample was taken from a pipe welded with Ar (100%) and solubilized at 1050 °C since it showed the worst corrosion behaviour.

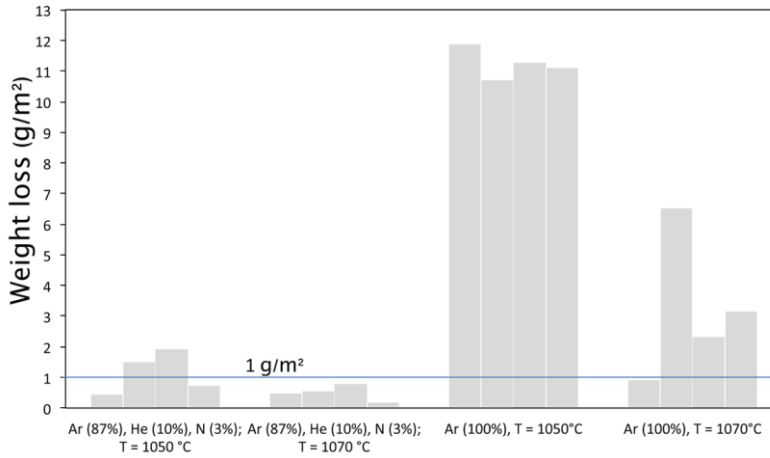

Fig. 8 Results of corrosion tests (ASTM A923, method C)

Fig. 9 shows the ESEM micrograph of the corroded sample after 6 h and 24 h from the beginning of the corrosion test.

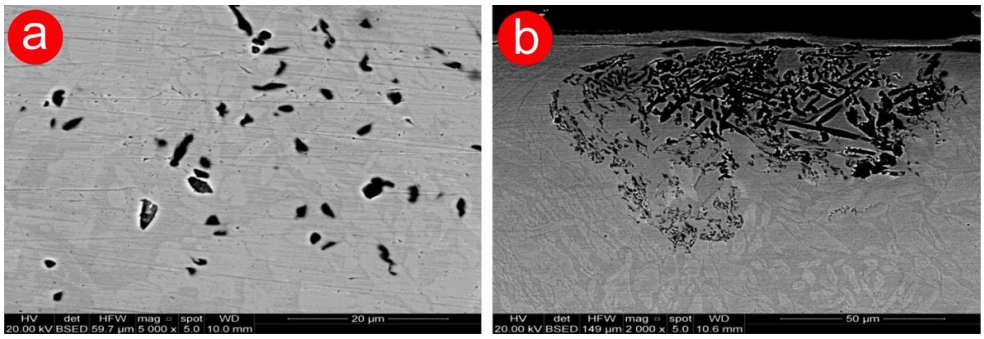

Fig. 9 SEM micrograph of the corroded joint after 6 h (a) and 24 h (b) from the beginning of the corrosion test

DOI 10.12776/ams.v24i2.1073 p-ISSN 1335-1532
e-ISSN 1338-1156

4 Discussion

The different obtained ferrite phase amounts in the three different zones of the bead (**Fig. 4**) of the as welded joints are related to Ni reached filler metal, cooling rates, shielding gas chemical composition and heating induced by the subsequent welding passes. In particular, the microstructure resulting by plasma welding is the most affected by the reheating induced by the successive two TIG welding passes (**Figs. 2b** and **3b**). This is the reason why only the fusion zones induced by plasma welding and inner TIG welding of as-welded joints are characterized by secondary austenite precipitation. It is observed also that the highest amount of ferrite in FZ2 (**Fig.1b**) is due to the absence of Ni-rich filler metal during welding.

Both secondary and primary austenite amount is higher in joints welded with SHG2 due to the nitrogen enrichment. From **Figs. 2** and **3** it is noted how nitrogen coming from SHG2 enhanced the austenite precipitation also in FZ2. Finally, the solution heat treatment at both 1050 °C and 1070 °C promotes a more balanced microstructure also in FZ3 (**Fig. 7**).

Intragranular colonies of secondary austenite showed a needle-shape morphology, being formed at temperatures higher than 650 °C [15-17] (**Figs. 5-6**).

The absence of nitrogen in SHG1 induced a higher amount of ferrite after each welding pass compared to the joints welded with SHG2. Such ferrite remains supersaturated with austenitizing elements that promote primary austenite growth and secondary austenite precipitation during the subsequent heating induced by both welding and heat treatment. The amount of ferrite phase transformed into secondary austenite was approximately quantified by measuring the area characterized by secondary austenite precipitation. The mean value of 20 fields at 200 magnifications for the samples heat treated at 1050 °C and welded with SHG1 and SHG2 was found 24±8.12 % and 8±4.29%, respectively.

It is noted from **Fig. 9** that the corrosion process attacks only the austenitic grains. In particular, it starts from secondary austenite (**Fig. 9a**) and than it involves primary austenite. As a matter of fact, in literature secondary austenite is found poorer in Cr, Mo and N compared to primary austenite [8] and thus more easily attacked by pitting corrosion. **Table 4** summarizes the estimated values of Cr and Mo in different zones of the microstructure of the sample showed in **Fig. 9** by EDS analysis (each value results from the average of ten measurements).

Table 4 Weight percentage of Cr and Mo in different zones of the capping welding pass induced FZ; joint welded with SHG1 and heat treated at 1050 °C

	Primary austenite	Secondary austenite	Ferrite around primary austenite	Ferrite around secondary austenite
Mo	3.32 ± 0.24	2.75 ± 0.13	4.06 ± 0.28	4.21 ± 0.18
Cr	21.72 ± 0.11	19.71 ± 0.21	22.77 ± 0.56	23.89 ± 0.26

In literature the resistance to pitting corrosion is estimated by means of the Pitting Resistant Equivalent Number (PREN) defined by the following equation [16]:

$$PREN = 1 \cdot \%Cr + 3.3 \cdot \%Mo + 16 \cdot \%N \quad (1.)$$

Even if it is not possible to measure the percentage of N with EDS, by neglecting in first approximation its repartition between the phases, it can be supposed from **Table 4** that secondary austenite is characterized by the lowest value of PREN [7].

DOI 10.12776/ams.v24i2.1073 p-ISSN 1335-1532
e-ISSN 1338-1156

The influence of shielding gas composition on corrosion properties of the joints can be quantified by calculation of the PREN value using data coming from spectrometer analysis without differentiating the single phases. As a matter of fact, data from spectrometer analysis on the capping zone of as-welded joints give PREN values of 33.65 and 36.9 for the joint welded with SHG1 and SHG2, respectively.

About the influence of the solution temperature on corrosion resistance of the joints, it was supposed that nitrogen redistributes in austenite during the heat treatment enriching the secondary austenite better at 1070 °C than 1050 °C. By comparing samples heat treated at 1050 and 1070 °C, a significant variation in the substitutional alloy elements (Cr, Mo) repartition between ferrite and austenite (primary and secondary) was not observed.

5 Conclusions

The effect of shielding gas composition and solution temperature on corrosion resistance of DSS welded joints was studied. The main results obtained can be summarized as follows:

1. Corrosion attack started from secondary austenite characterized by the lower amount of the substitutional elements, Cr and Mo.
2. Only the samples welded with the mixture of Ar (87%), He (10%), N (3%) as shielding gas and solution heat treated at 1070 °C have passed the corrosion test completely. This was attributed to both the nitrogen alloy enrichment and repartition between secondary and primary austenite during the solution heat treatment.
3. Better corrosion resistance of the joints welded with SHG2 compared to those welded with SHG1 was attributed to the nitrogen enrichment that increases the PREN value and reduces the secondary austenite amount.

References

[1] J. Charles, S. Bernhardson: The duplex stainless steels: materials to meet your needs, In.: Duplex Stainless Steels ’91, Beaune (France), Les Editions de Physique, 1991, p. 3-48.
[2] H.D. Solomon, T.M. Devine Jr.: Duplex stainless steels: a tale of two phases. In: Conference of the Duplex Stainless Steels; 1982; Ohio. Ohio: ASM; 1982, p. 693-756.
[3] J.-O. Nilsson: Materials Science and Technology, Vol. 8, 1992, No 8, p. 685-700, doi: 10.1179/mst.1992.8.8.685
[4] R. Gunn: Duplex stainless steels-Microstructure, properties and applications, Abington Publishing, Cambridge, 1997, doi:10.1533/9781845698775
[5] S. Pak, L. Karlsson: Scandinavian Journal of Metallurgy, Vol. 19, 1990, p. 9-13, doi: not found (Pak S. and Karlsson L.: Optimizing the properties of duplex stainless weld metals by addition of nitrogen, Scandinavian Journal of Metallurgy, 1990, vol. 19, pp. 9-13)
[6] J.-O. Nilsson, A. Wilson: Materials Science and Technology, Vol. 9, 1993, p. 545-554, doi: 10.1179/mst.1993.9.7.545
[7] J.-O. Nilsson, L. Karlsson, J.-O. Andersson: Materials Science Technology, Vol. 11, 1995, p. 276-283, doi: 10.1179/mst.1995.11.3.276
[8] P. Sathiya, S. Aravindan, R. Soundararajan, A. Noorul Haq: Journal of Materials Science, Vol. 44, 2009, p. 114-121, doi: 10.1007/s10853-008-3098-8
[9] S. Hertzman, P. Ferreira, B. Brolund: Metallurgical and Materials Transactions A, Vol. 28A, 1997, p. 277-285, doi: 10.1007/s11661-997-0130-6
[10] P. Ferro, A. Fabrizi, F. Bonollo: Acta Metallurgica Sinica (English Letters), Vol. 29, 2016, No 9, p. 859-868, doi: 10.1007/s40195-016-0462-6

[11] P. Ferro, F. Bonollo: Metallurgical and Materials Transactions A, Vol. 43A, 2012, No 4, p. 1109-1116, doi: 10.1007/s10853-010-4311-0
[12] R. Cervo, P. Ferro, A. Tiziani, F. Zucchi: Journal of Materials Science, Vol. 45, 2010, p. 4378-4389.
[13] Z. Zhang et al.: Corrosion Science, Vol. 62, 2012, p. 42–50, doi: 10.1016/j.corsci.2012.04.047
[14] Y. Yang et al.: Corrosion Science, Vol. 65, 2012, p. 472–480, doi: 10.1016/j.corsci.2012.08.054
[15] J. Nowacki, A. Lukojc: Journal of Materials Processing Technology, Vol. 164, 2005, No 165, p. 1074-1081, doi: 10.1016/j.jmatprotec.2005.02.243
[16] British stainless steels association web site: [11.4.2018] https://www.bssa.org.uk/topics.php?article=111

Acknowledgments
Authors thank RIVIT S.p.A. (Caltrano (VI), IT) for the materials and welding tests.